JOURNAL OF CHEMICAL INFORMATION AND MODELING

Article

pubs.acs.org/jcim

Molecular Modeling of the 3D Structure of 5-HT$_{1A}$R: Discovery of Novel 5-HT$_{1A}$R Agonists via Dynamic Pharmacophore-Based Virtual Screening

Lili Xu,[†,§] Shanglin Zhou,[‡,§] Kunqian Yu,[‡,§] Bo Gao,[∥] Hualiang Jiang,*[,‡] Xuechu Zhen,*[,∥] and Wei Fu*[,†]

[†]Department of Medicinal Chemistry & Key Laboratory of Smart Drug Delivery, Ministry of Education, School of Pharmacy, Fudan University, Shanghai 201203, China

[‡]State Key Laboratory of Drug Research, Shanghai Institute of Materia Medica, Chinese Academy of Sciences, Shanghai 201203, China

[∥]Department of Pharmacology, Soochow University College of Pharmaceuticals Sciences, Suzhou 215123, China

Supporting Information

ABSTRACT: The serotonin receptor subtype 1A (5-HT$_{1A}$R) has been implicated in several neurological conditions, and potent 5-HT$_{1A}$R agonists have therapeutic potential for the treatment of depression, anxiety, schizophrenia, and Parkinson's disease. In the present study, a homology model of 5-HT$_{1A}$R was built based on the latest released high-resolution crystal structure of the β_2AR in its active state (PDB: 3SN6). A dynamic pharmacophore model, which takes the receptor flexibility into account, was constructed, validated, and applied to our dynamic pharmacophore-based virtual screening approach with the aim to identify potential 5-HT$_{1A}$R agonists. The obtained hits were subjected to 5-HT$_{1A}$R binding and functional assays, and 10 compounds with medium or high K_i and EC$_{50}$ values were identified. Among them, **FW01** (K_i = 51.9 nM, EC$_{50}$ = 7 nM) was evaluated as the strongest agonist for 5-HT$_{1A}$R. The active 5-HT$_{1A}$R model and dynamic pharmacophore model obtained from this study can be used for future discovery and design of novel 5-HT$_{1A}$R agonists. Also, by integrating all computational and available experimental data, a stepwise 5-HT$_{1A}$R signal transduction model induced by agonist **FW01** was proposed.

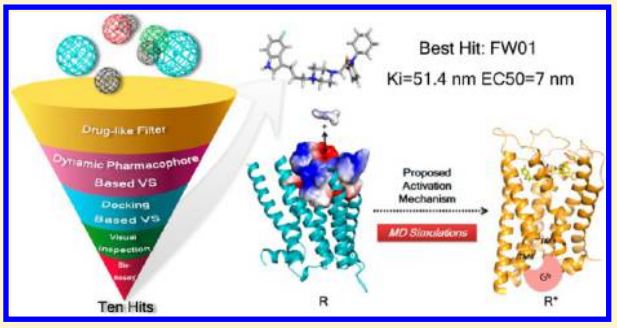

INTRODUCTION

Serotonin (5-hydroxytrptamine, 5-HT), one of the most important neurotransmitters in the brain, was involved in most of the human behavioral and neuropsychological processes, modulating mood, cognition and memory, feeding, sexuality, sleep, and pain, etc.[1] Abnormal 5-HT transmission is associated with pathogenesis of psychiatric disorders and neurodegenerative disorders. To date, at least 16 serotonin receptor subtypes have been cloned which are grouped into seven subfamilies (5-HT$_{1-7}$) based on their different signaling mechanisms.[2] Among them 5-HT$_{1A}$R was the first one to be fully sequenced and widely studied. Its involvement in anxiety and depression has long been documented.[3−5] Growing evidence has revealed new therapeutic applications of 5-HT$_{1A}$R in the treatment of schizophrenia,[6] Parkinson's disease,[7] and neural damage.[8]

Accordingly, intensive efforts have been made to explore the therapeutic application of 5-HT$_{1A}$R agonists in the past three decades.[9−11] Representative 5-HT$_{1A}$R agonists include R-8-OH-DPAT (full agonist; widely used agonistic tool drug),[12] Buspirone (partial agonist; anxiolytic),[13] Vilazodone (SSRI/5-HT$_{1A}$R partial agonist; antidepressant),[14] Aripirazole (mixed receptor profile with 5-HT$_{1A}$R agonistic activity; atypical antipsychotic),[15] F-13640 (highly selective and effective full agonist; undergoing clinical trials for the treatment of pain)[16] (Table 1). Given the rising interest on 5-HT$_{1A}$R agonists, new

Table 1. Pharmacophore Model Validation Using Statistical Parameters

parameter	value
total compounds in database (D)	1000
total number of actives in database (A)	25
total hits (Ht)	33
active hits (Ha)	21
% yield of actives	63.6
% ratio of actives in the hit list	84
enrichment factor or enhancement (E)[a]	25.45
false negatives	4
false positives	12
GH score (goodness of hit list)[a]	0.68

[a]E = (Ha/Ht)/(A/D); GH = [((Ha/4HtA)(3A +Ht))(1((HtHa)/(DA)))], GH score of 0.6−0.7 indicates a good model.

Received: August 14, 2013
Published: November 18, 2013

ACS Publications © 2013 American Chemical Society

chemical entities with high efficacy and good pharmacokinetic profiles are still limited. Most reported molecules were originated from several widely studied structural classes such as indolylalkylamines and arylpiperazines. Though ligand-based approach can lead to molecules with high and even super high 5-HT_{1A}R affinity more easily, the diversification of 5-HT_{1A}R agonist scaffolds is impaired. Also, the lack of accurate 5-HT_{1A}R structure is another significant impediment.

Thanks to the great advances in X-ray crystallography, the advent of high-resolution crystal structure of the β_2AR in its active state (PDB: 3SN6)[17] provides us with a good opportunity to model the 3D structure of 5-HT_{1A}R accurately. Based on the constructed model of 5-HT_{1A}R, we further adopted dynamic pharmacophore-based virtual screening approach for the discovery of novel 5-HT_{1A}R agonists. In this approach, a dynamic pharmacophore model was developed and applied to search compounds. This dynamic pharmacophore-based virtual screening (DPB-VS) method, first developed by Heather A. Carlson,[18] has been successfully applied to systems like HIV-1 integrase,[19] fatty acid amide hydrolase (FAAH),[20] and Histone Deacetylase 8 (HDAC8).[21] Practices have proved that dynamic pharmacophore models perform better than static ones for they take the flexibility of active site into account. In our study, a 100 ns molecular dynamic simulation of the R-8-OH-DPAT-5-HT_{1A}R complex was conducted in order to generate a collection of representative agonistic conformations, and the active site of 5-HT_{1A}R was then mapped by using five types of chemical probes. Followed by cluster analysis of features, a dynamic pharmacophore model for 5-HT_{1A}R was built. Compounds retrieved from DPB-VS were further subjected to docking based-virtual screening (DB-VS). Finally, a set of compounds displaying agonistic activity at 5-HT_{1A}R were revealed by biological tests. Among them, **FW01** displays the strongest agonistic activity toward 5-HT_{1A}R. Furthermore, the binding mode of **FW01** and 5-HT_{1A}R was investigated by means of molecular docking and dynamics simulations study. Finally, a stepwise 5-HT_{1A}R signal transduction model hereof was proposed.

MATERIALS AND METHODS

Homology Modeling. The amino acid sequence of 5-HT_{1A}R was downloaded from the UniProtKB database (Entry code: P08908), and sequence similarity search was performed using the NCBI BLAST server.[22] The lately disclosed active-state structure (PDB code: 3SN6)[17] of β_2AR was selected as the template to construct the agonistic conformation of 5-HT_{1A}R. Sequence alignment of 5-HT_{1A}R and β_2AR was carried out using the ClustalX 2.0 program.[23] Homology modeling was performed with Discovery Studio 3.5 (hereafter abbreviated to DS).[24] Fifty models were generated after loop refinement, and the one with the lowest Discrete Optimized Protein Energy (DOPE) score was submitted to energy minimization (1000 steps steepest descent with backbone constrained). The PROCHECK program[25] was used to evaluate the stereochemical quality of 5-HT_{1A}R.

Molecular Docking. GoldSuite 5.0[26] was employed to conduct flexible docking. Briefly, the binding pocket was defined to include all residues within 10.0 Å of Cγ carbon atom in conserved D3.32 (superscripts refer to Ballesteros-Weinstein numbering[27]). Full flexibility was allowed for ligands. The number of genetic algorithm (GA) runs was set to 10, and GoldScore was selected as the scoring function. The top-ranking solutions were visually inspected by considering favorable interactions with the key residues demonstrated by available mutagenesis studies. The most reasonable complex was then submitted to QM/MM minimization encoded in DS to eliminate bad contacts. The ligand, together with the side chain atoms of D3.32 and S5.42, was included in the QM region for a quantum calculation using Dmol3, and the rest was handled by CHARMm force field in the MM region.

Molecular Dynamics Simulation. The MD simulations were performed using the GROMACS 4.5.1 package.[28] The R-8-OH-DPAT-5-HT_{1A}R complex was embedded in an explicit hydrated POPC membrane bilayer. Protein was inserted according to the InflateGRO methodology described by Kandt,[29] reaching an area per lipid of ~75 Å. The system was then solvated with SPC waters in a 80 × 80 × 86 Å box, and bad waters were removed. A neutralized system with an ionic concentration of 154 mmol/L was reached by randomly replacing water molecules with the proper number of Na^+ and Cl^-. The resulting system for R-8-OH-DPAT-5-HT_{1A}R contains 35156 atoms. The Berger lipid parameter was used for the POPC molecules[30] in combination with GROMOS96 53A6 force field for the protein. The molecular topology of R-8-OH-DPAT was prepared with PRODRG,[31] and the partial charge was calculated by using the ChelpG method implemented in the Gaussian 09[32] with the DFT/B3LYP/6-311g** basis set. The other two systems of the **FW01**-5-HT_{1A}R complex and the ligand-free 5-HT_{1A}R in its inactive state were set up in a similar way.

Prior to MD simulation, energy minimizations were performed to eliminate poor contacts. After 1000 steps of steepest decent and 200 steps of conjugate gradient energy minimization, the maximum force was converged to less than 10.00 kcal/mol/Å. After each system was heated gradually from 0 to 310 K by v-scale thermostat, a 1-ns NPT equilibration was performed with protein and ligand restrained, using the Nose-Hoover thermostat to keep the temperature at 310 K, and the Parrinello-Rhaman method to maintain a constant pressure of 1 bar. 500-ps unrestrained equilibration ran afterward. Periodic boundary conditions were applied. A time step of 2.0 fs was employed. All bonds were constrained by the LINCS algorithm. Electronic interactions were calculated using the Partical-Mesh Ewald (PME) algorithm. A 100-ns production run was carried out for the R-8-OH-DPAT-5-HT_{1A}R complex system and 100 ns for the **FW01**-5-HT_{1A}R complex and the ligand-free 5-HT_{1A}R systems with coordinates saved every 2 ps for later analysis.

Cluster Analysis. The 5000 protein conformations extracted every 20 ps from the trajectory of the R-8-OH-DPAT-5-HT_{1A}R complex simulation system were clustered based on root-mean-square deviation (RMSD) of the conformations using the GROMOS conformational cluster analysis method as implemented in the GROMACS. A cutoff value of 1.2 Å was employed as the criteria to assign a cluster, generating a total of 36 clusters. The representative structures from the top 5 popular clusters (-I, -II, -III, -IV, -V) were used to build the dynamical pharmacophore model.

Active Site Mapping and PharmacophoreModel Generation. The GRID 22 program[33] was used to map the active sites of the five representative structures of 5-HT_{1A}R to detect energetically favorable interactions with the following probes: negative ionizable (COO−), positive ionizable (N1+), hydrogen-bond acceptor (O), hydrogen-bond donor (N1), and hydrophobic probes (DRY). The output from the GRID calculations was visualized and superimposed using VMD.[34]

dx.doi.org/10.1021/ci400481p | J. Chem. Inf. Model. 2013, 53, 3202−3211

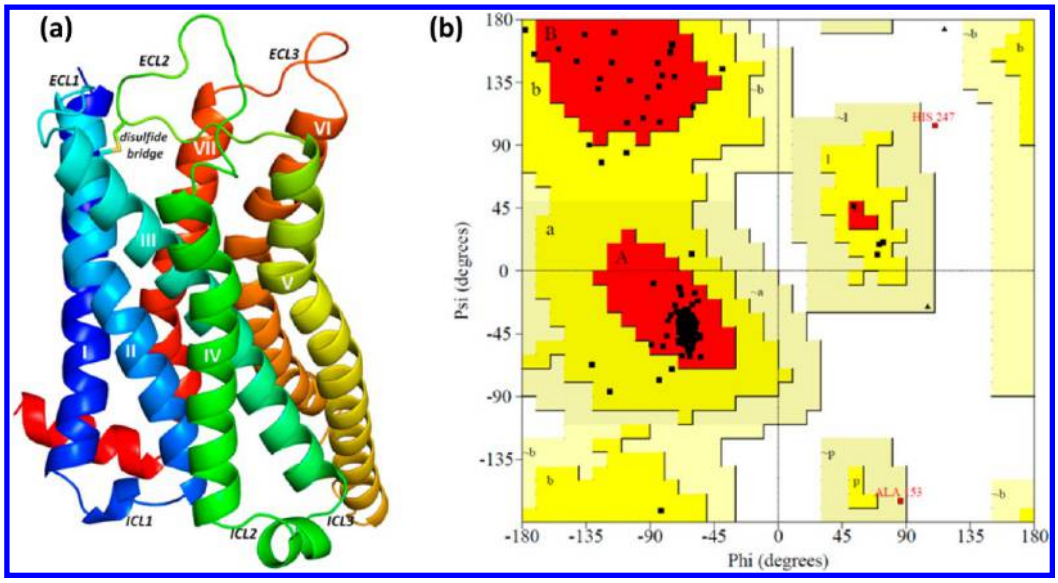

Figure 1. Homology model of 5-HT_{1A}R. a, Homology model of 5-HT_{1A}R in cartoon representation. b, Ramachadran plot calculated for the 5-HT_{1A}R model.

For each of the five probes, the grid points were superimposed to identify clusters. Corresponding pharmacophore feature was generated in situ at the geometric center of each cluster with the tolerance volume determined by the radius of gyration of corresponding cluster. For the pharmacophore model developed in this study, clusters were selected based on the binding mode of R-8-OH-DPAT in 5-HT_{1A}R. Clusters of the N1+ probe that were within a distance of 3 Å from the conservative residue D3.32 were selected; clusters of both O and N1 probes within a hydrogen-bonding distance from the conserved S5.42 were selected; two hydrophobic clusters of DRY probe within a distance of 5 Å from conserved F6.51, F6.52, and W7.40 were selected. Thus, a four-feature pharmacophore model of 5-HT_{1A}R was generated. Moreover, to reduce the false positive rate of virtual screening, three excluded volumes right at the position of side chains of D3.32, F6.51, and Y7.43 were added.

Dynamic Pharmacophore-Based Virtual Screening. In our virtual screening approach, the *Ligand Pharmacophore Mapping* protocol embedded in DS was employed to retrieve potential molecules from Maybridge and Specs chemical databases[35] with the dynamic pharmacophore model as a 3D query. The two databases, each containing 61623 and 166778 compounds, were filtered by Lipinski's "Rule of Five"[36] to create druglike databases in advance using *Prepare Ligands* protocol. For each molecule in the database, a maximum of 100 conformers with an energy threshold of 20 kcal/mol were generated using FAST algorithm. The Best and Flexible mapping option was adopted. Compounds were required to match at least three features of input pharmacophore (Fit Value $\geq$2.95). Hits were then subjected to GOLD docking. Specially, the automatic genetic algorithm search option was used, and the search efficiency was set at 30% which is recommended for virtual screening. Other parameters were the same as described before in the molecular docking section. Outcome solutions were sorted by GoldScore. Compounds with GoldScore >45 were retained for further visual inspection.

Binding Assays. All the selected compounds were subjected to competitive binding assays for 5-HT_{1A} receptor, using membrane preparation obtained from stable transfected CHO cells as previously described by our laboratory.[37,38] First, the ability at a concentration of 10 μM to inhibit the binding of a tritiated radioligand to the corresponding receptor was tested. Compounds that inhibited binding by more than 90% were further assayed at six or more concentrations, ranging above and below IC_{50}. The K_i values were calculated using the following equation: $K_i = IC_{50}/(1+C/K_d)$. [^{3}H]5-HT was used as the standard radioligand for 5-HT_{1A} receptor. Duplicate tubes were incubated at 30 °C for 50 min with increasing concentrations (1 nM to 100 μM) of each compound and with 0.7 nM [^{3}H]5-HT in a final volume of 200 μL of binding buffer containing 50 mM Tris and 4 mM $MgCl_2$ (pH 7.4). Nonspecific binding was assessed by parallel incubations with 10 μM 5-HT. The reaction was started by addition of membranes (15 μg/tube) and stopped by rapid filtration through a Whatman GF/B glass fiber filter and subsequent washing with cold buffer [50 mM Tris and 5 mM ethylenediaminetetraacetic acid (EDTA) (pH 7.4)] using a Brandel 24-well cell harvester. Scintillation cocktail was added, and the radioactivity was determined in a MicroBeta liquid scintillation counter. The IC_{50} and K_i values were calculated by nonlinear regression (PRISM, Graphpad, San Diego, CA) using a sigmoidal function.

[^{35}S]-GTPγS Assays. The [^{35}S]GTPγS binding assay was performed at 30 °C for 30 min with 10 μg of membrane protein in a final volume of 100 μL with various concentrations of the compounds. The binding buffer contained 50 mM Tris (pH 7.5), 5 mM $MgCl_2$, 1 mM ethylenediaminetetraacetic acid (EDTA), 100 mM NaCl, 1 mM DL-dithiothreitol (DTT), and 40 μM guanosine triphosphate (GDP). The reaction was initiated by the addition of [^{35}S]GTPγS (final concentration of 0.1 nM). Nonspecific binding was measured in the presence of 100 μM 5′-guanylimidodiphosphate (Gpp(NH)p). The reaction was terminated by the addition of 1 mL of ice-cold washing buffer (50 mM Tris, 5 mM $MgCl_2$, 1 mM EDTA, 100 mM NaCl) and was rapidly filtered with GF/C glass fiber filters (Whatman) and washed three times. Radioactivity was determined by liquid scintillation counting.

Chart 1. Representative 5-HT$_{1A}$R Agonists

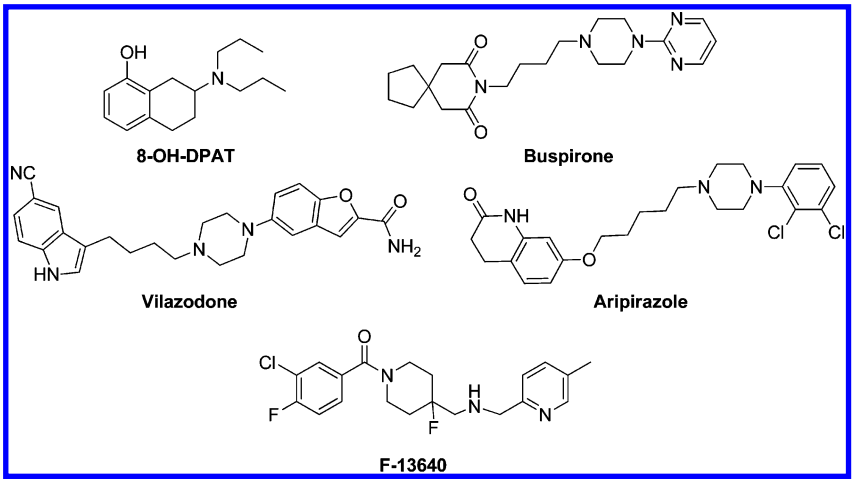

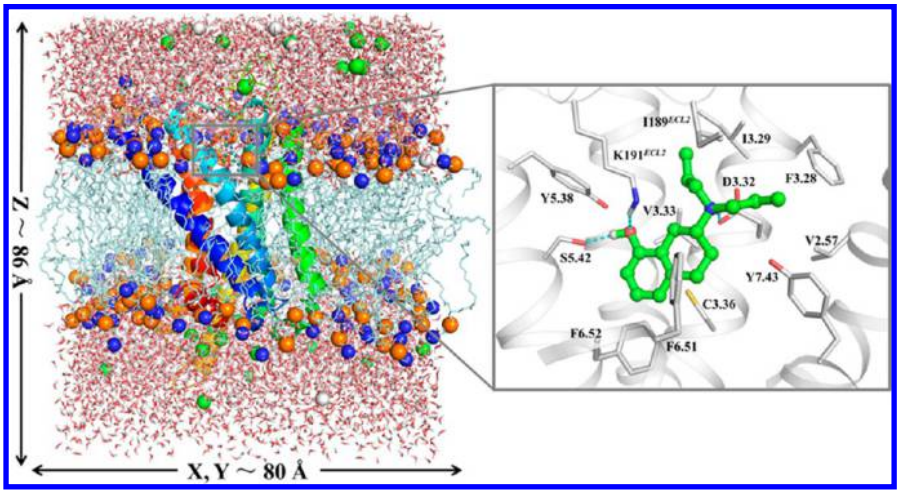

Figure 2. Side view of the R-8-OH-DPAT-5-HT$_{1A}$R complex embedded in a hydrated POPC lipid bilayer (left). 5-HT$_{1A}$R is shown in cartoon representation with R-8-OH-DPAT in the upper center. Water molecules and lipid molecules are shown in sticks; and choline N (blue), P atoms (orange) and Na^+ (gray), CL^- (green) ions are represented in spheres. The detail of the binding mode of R-8-OH-DPAT with 5-HT$_{1A}$R is amplified (right). 5-HT$_{1A}$R is shown in gray ribbons and R-8-OH-DPAT in green ball and sticks. Hydrogen bonds are depicted in dotted lines.

RESULTS AND DISCUSSION

3D Structure of the 5-HT$_{1A}$R Model. Sequence alignment indicated that the sequence identity in the transmembrane region is ~45% between 5-HT$_{1A}$R and β_2AR. The most recently disclosed crystal structure of the β_2AR-Gs complex in active state (PDB Code: 3SN6) was the optimal template to construct the 5-HT$_{1A}$R model. Therefore, it was expected that our model represents the active state of the receptor. Figure S1 shows the final sequence alignment of 5-HT$_{1A}$R to the template. The PROCHECK statistics showed that 99.2% of the residues in the 5-HT$_{1A}$R model (Figure 1a) were either in the most favored or in the additionally allowed regions of the Ramachandran plot; only one residue in the loop is located in the disallowed region (Figure 1b), suggesting that the overall main chain and side chain conformations are reasonable. Besides, several structural features present in the 5-HT$_{1A}$R model are characteristic of active conformations of family A GPCRs:[39] the broken Arg3.50-Glu6.30 ionic lock due to a large separation of TM3-TM6 in the cytoplasmic ends and Tyr7.53 of the NPxxY motif (so-called "Tyrosine Toggle Switch") extending into the protein interior. Compared to previously reported 5-HT$_{1A}$R models which were built based on the crystal structure of β_2AR bound to the partial inverse agonist carazolol (PDB Code: 2RH1) or bovine rhodopsin (PDB Code: 1F88), our model was built taking the active state conformation of the β_2AR-Gs complex as template and represents the active conformation binding with agonists. Thus it is suitable for the investigation of discovery of 5-HT$_{1A}$R agonists.

8-OH-DPAT (Chart 1), a prototypical 5-HT$_{1A}$R agonist, has been extensively used for pharmacological studies.[40] R-8-OH-DPAT displays higher efficacy than its S-counterpart and acts as a full 5-HT$_{1A}$R agonist, thus it was chosen herein to induce active receptor conformations. The predicted binding mode (Figure 2, right) is quite consistent with all the available experimental studies: the protonated nitrogen forms a salt bridge with the negatively charged D3.32, and the hydroxyl group is involved in the hydrogen bonds with Ser5.42 and Lys191 (ECL2). The importance of conserved D3.32 and S5.42 for 5-HT binding to 5-HT$_{1A}$R was supported by a site-directed mutagenesis study.[41] Additionally, F6.51 and F6.52 are participated in the aromatic stacking with R-8-OH-DPAT. The two phenylalanine residues in TM6 contribute to hydrophobic interaction and were proved to be crucial for ligand binding in the case of the dopamine D2 receptor.[42] The di-*n*-propyl substituent was found stretched in the hydrophobic

dx.doi.org/10.1021/ci400481p | J. Chem. Inf. Model. 2013, 53, 3202−3211

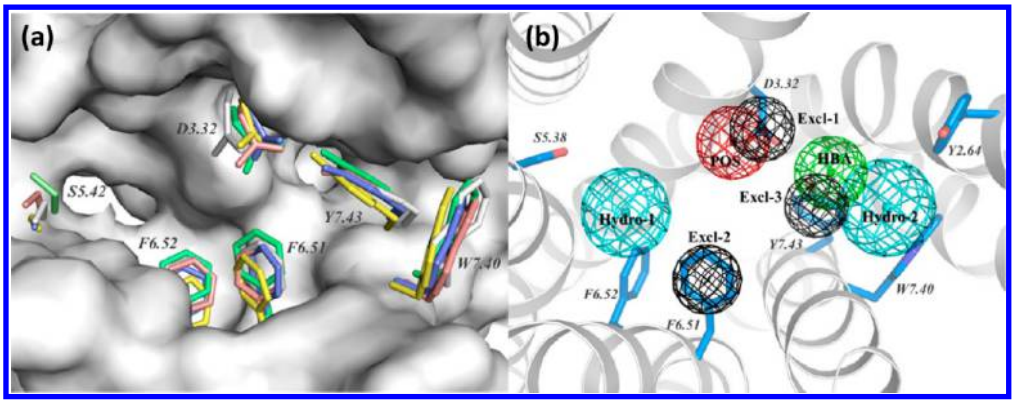

Figure 3. a, Superimposition of the five major 5-HT_{1A}R conformations obtained from 100 ns MD simulation. Cluster-I representative structure is shown in white surface. Conserved residues in the binding pocket of Cluster -I, -II, -III, -IV, and -V representative conformations are colored separately in white, blue, green, yellow, and pink. b, Top view of the pharmacophore model mapped into the active pocket of 5-HT_{1A}R (only Cluster-I representative structure was shown for clarity). Two hydrophobic elements (Hydro-1, -2), a positive ionizable element (POS), a hydrogen bond acceptor element, and three excluded volumes (Excl-1, -2, -3) are represented in cyan, red, green, and black spheres, respectively.

pocket (enclosed by ECL2 and the extracellular segments of TM-3, -7) which is also typical among dopamine receptors. MD simulation was started with the obtained R-8-OH-DPAT-5-HT_{1A}R complex embedded in a hydrated POPC lipid bilayer (Figure 2, left). During the simulation 8-OH-DPAT was constantly trapped in the binding pocket of 5-HT_{1A}R. Taken together, our predicted 5-HT_{1A}R model is credible, and conformations generated from MD simulation shall stand for active states of the receptor.

The Dynamic Pharmacophore Model Generation. Five representative structures obtained from clustering were used to represent the flexibility of 5-HT_{1A}R and to build the dynamic pharmacophore model. GRID probed the active site with five types of functional groups (COO-, N1+, O, N1, and DRY) to find the most favorable regions for them to interact with the protein, generating a total of 25 interaction maps (5 for each protein conformation), and they were overlaid based on the superimposition of the five major 5-HT_{1A}R conformations (Figure 3a). Backbone atoms RMSD of representative structures in each Cluster (II, III, IV, V) to the major conformer (Cluster I) is 1.48 Å, 1.38 Å, 1.74 Å, 1.39 Å, respectively. On the basis of site-directed mutagenesis data and computational studies available in the literature,[41,43,44] i.e. hydrogen bond contacts with D3.32, Ser5.42, T5.43, N7.39, Y7.43 and $\pi-\pi$ stacking interactions with Y2.64, W6.48, F6.51, F6.52, W7.40, Y7.43 are crucial for 5-HT_{1A}R agonist binding, only the features complementary to these key residues were considered. Generally, a positive ionizable feature (POS) was chosen to target the negatively charged carboxylic side chain of D3.32, the hydrogen-bond acceptor (HBA) feature located close to Y7.43 was retained, and large clusters found in two hydrophobic regions, which are surrounded by TM5/TM6 and TM2/TM7/ECL2, were combined into two hydrophobic features (HYDRO-1, -2), respectively. Whereas, clusters of COO- probes were discarded due to the electrostatic repulsion between COO- and negatively charged residues in the binding site of 5-HT_{1A}R (Figure 7), and the hydrogen-bond donor feature adjacent to S5.42/T5.43 was also omitted for it partially overlapped with HYDRO-1. Thus, a four-feature pharmacophore model was produced (Figure 3b). Three exclusion volumes (Excl-1, -2, -3) were *in situ* generated from the side chains of the conserved residues D3.32, F6.51, and Y7.43.

Validation of a Pharmacophore Model. The Güner-Henry (GH) scoring method[45] was used to assess the ability of our pharmacophore model to discriminate a small number of known active molecules against a greater number of decoy molecules in the database. The decoy set contains a total of 1000 compounds, including 25 highly active 5-HT_{1A}R agonists taken from ChEMBL database,[46] and 975 matched decoys generated from online DUD-E (Directory of Useful Decoys, Enhanced) tool.[47] The pharmacophore model was used to screen the decoy set employing the BEST flexible searching method. A set of statistical parameters were set to analyze the result (Table 1). 33 compounds were retrieved as hits with a hit rate of 63.6%. In addition, the pharmacophore model showed an enrichment factor of 25.45 and a GH score of 0.68, indicating the good quality of our model.

Database Searching and Bioassay Results. The validated pharmacophore model was then used as a 3D query to screen Maybridge and Specs databases, of which nondruglike compounds were rejected. A total of 18,976 compounds obtained from PB-VS were docked into the representative structure of 5-HT_{1A}R in the biggest cluster. 1500 compounds with GoldScore >45 were extracted for visual inspection. Compounds that form favorable interactions with key residues in the active site such as D3.32, S5.42, F6.51, and F6.52 were chosen, and those with unreasonable binding modes were discarded. At last, a total of 45 compounds, 16 from Specs and 29 from Maybridge, were selected to purchase from their suppliers. The flowchart of hybrid searching approach was shown in Figure 4.

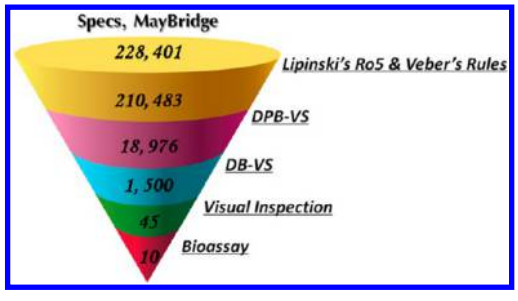

Figure 4. Workflow of dynamic pharmacophore-based virtual searching approach.

dx.doi.org/10.1021/ci400481p | J. Chem. Inf. Model. 2013, 53, 3202−3211

Chart 2. Chemical Structures of 10Hit Compounds

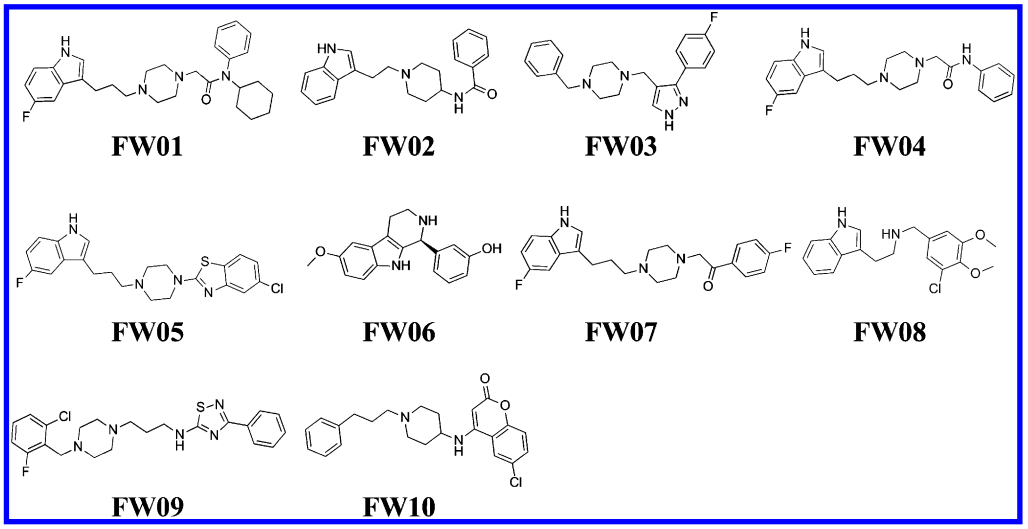

Table 2. Summary of the Molecular Properties, Fit Values, GoldScores, and Biological Evaluations of Hit Compounds

hit	MW	HBA	HBD	AlogP	fit value	GoldScore	[^{3}H]5-HT[a] K_i (nM)	[^{35}S]GTPγS[b] EC_{50} (nM)
FW01	476.6	5	1	5.84	3.60	50.7	51.9 ± 16.4	7
FW02	347.5	4	2	3.35	3.74	47.4	70.5 ± 14.8	77
FW03	350.4	4	1	4.04	2.96	48.5	96.5 ± 13.1	404
FW04	394.5	5	2	3.77	3.40	45.7	103.5 ± 23.4	128
FW05	429.0	4	1	6.10	3.17	50.7	123.6 ± 32.0	534
FW06	294.3	4	3	3.27	3.10	52.0	133.4 ± 9.7	434
FW07	397.5	4	1	4.60	3.70	45.2	225.2 ± 20.2	340
FW08	344.8	4	2	4.20	3.15	54.4	294.9 ± 5.0	572
FW09	446.0	5	1	4.74	3.50	59.2	320.1 ± 76.9	597
FW10	396.9	4	1	4.27	3.48	50.1	351.7 ± 19.0	ND[c]
5-HT							1.8 ± 0.1	3

[a]Binding data are the mean values of five to six individual experiments with 5-HT$_{1A}$ receptors each done in triplicate. [b]Agonist stimulated [^{35}S]GTPγS binding derived from a mean curve out of five experiments with human 5-HT$_{1A}$ receptors stably expressed in CHO cells. [c]ND = not determined.

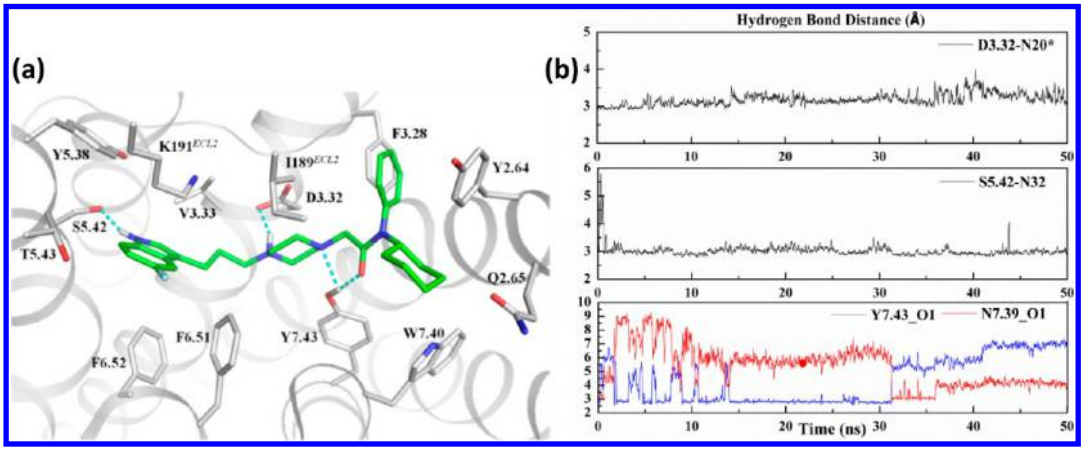

Figure 5. a, Predicted binding mode of compound **FW01** (green, sticks) with 5-HT$_{1A}$R (white, cartoon). Hydrogen bonds are illustrated as cyan dotted lines. b, Evolution of the hydrogen bond distances between compound **FW01** and 5-HT$_{1A}$R during the 50 ns simulation. * Distance was calculated between the centroid of two equal carboxylic oxygen atoms of D3.32 and the protonated nitrogen atom (N20) in **FW01**.

The competitive binding assays were carried out for the purchased 45 compounds. The inhibitory potency was tested with each compound at a fixed concentration of 10 μM. Ten compounds (**FW01-FW10**, Chart 2) showed an inhibition rate greater than 90%, and their K_i values were calculated. Table 2 summarizes the results of virtual screening and corresponding binding assays. Out of the 10 compounds tested, 5 compounds displayed K_i values of less than 100 nM. Novelty confirmation revealed that these compounds were not reported for the affinity to 5-HT$_{1A}$R. To explore agonistic or antagonistic properties of these compounds, compounds **FW01-FW10** were subjected to [^{35}S]-GTPγS function assays at 5-HT$_{1A}$R. As we

dx.doi.org/10.1021/ci400481p | J. Chem. Inf. Model. 2013, 53, 3202−3211

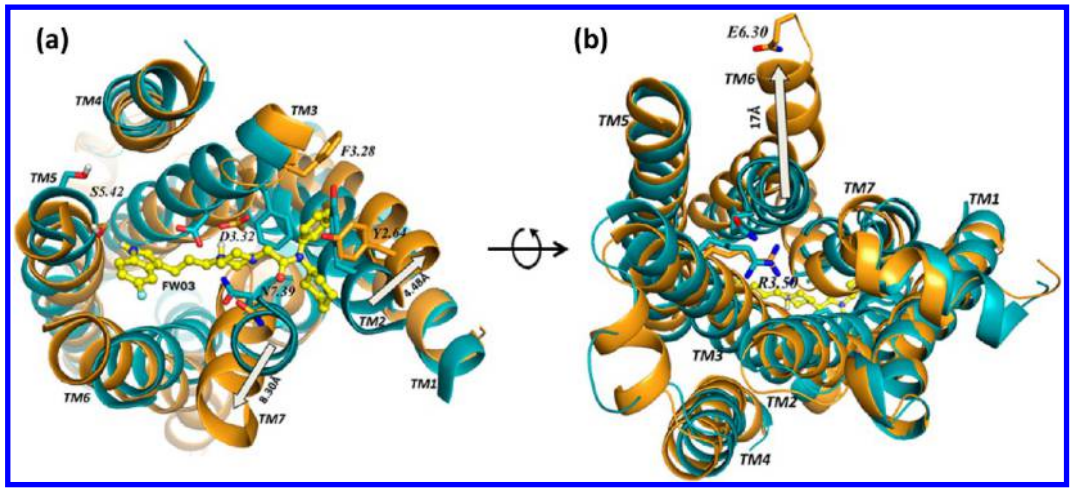

Figure 6. Comparison of superimposed structures - inactive 5-HT_{1A}R structure (blue cartoon) and agonist (**FW01**, yellow ball and sticks)-bound active 5-HT_{1A}R structure (orange cartoon). a, Extracellular view showing outward movements of TM2 and TM7 by ca. 4.48 Å and 8.3 Å, respectively, and modest structural changes of other TMs. b, Cytoplasmic view showing large outward movement of TM6, ca. 17 Å.

expected, they are all turned out to be 5-HT_{1A}R agonists (Table 2).

Through chemical structure analysis, these identified potential 5-HT_{1A}R agonists all contain common sp^3 nitrogen, which is universe among GPCRs ligands, and aromatic rings attached to different types of scaffolds. Accordingly, these compounds can well match our proposed dynamic pharmacophore model. The most potential hit **FW01** (EC_{50} = 7 nM) attracted our interest, which turns out to display comparable intrinsic activity to 5-HT; therefore, it was chosen as the lead compound for the analogue optimization, and a series of strong agonists with K_i < 10 nM was already obtained (unpublished work).

Binding of FW01 with 5-HT_{1A}R. To get structural insights into the strong agonistic mechanism of **FW01**, its binding mode with 5-HT_{1A}R was predicted by molecular docking (Figure 5a), and the obtained complex was subjected to 100 ns molecular dynamics simulation. **FW01**, with a stretched scaffold, lies in the same pocket as R-8-OH-DPAT. The conserved salt bridge interaction with D3.32 and hydrogen bond with Ser5.42 were kept. The other nitrogen atom in the\ piperazine ring and the carbonyl group can be both potentially involved as an acceptor in the hydrogen bond with Y7.43. Besides, adjacent residues like Y5.38 and K191 located in ECL2 form favorable $\pi-\pi$ and cation-π interactions with the indole ring, respectively. In addition, the benzene ring in the tail is sandwiched between the side chains of F3.28 and Y2.64.

During the simulation time, the salt bridge between D3.32 and **FW01** remains stable (Figure 5b). S5.42 interacts tightly with the nitrogen atom of the indole ring (Figure 5b). While the other hydrogen bond between Y7.43 and the carbonyl group fluctuates and disappears after ~31 ns (Figure 5b). N7.39, which locates one turn above Y7.43, was involved in as a competitive H-bond partner (Figure 5a). Thus N7.39 might also play an important role in facilitating the agonistic conformation of 5-HT_{1A}R. The results suggest that residues Y2.64, F3.28, Y5.38, Y7.39, Y7.43, and K191 also contribute to the binding of the agonist and activation of the receptor.

Agonist-Induced Structural Changes in 5-HT_{1A}R. We next compared the structure of active and inactive 5-HT_{1A}R. Several major conformational changes are found both at the cytoplasmic face and the extracellular side of the receptor (Figure 6). The extracellular part of TM2 and TM7 undergoes large-scale displacements—a 4.48 Å outward movement of TM2 and an 8.3 Å outward movement of TM7 (Figure 6a), which are not demonstrated in current available crystal structures of GPCRs. The most significant outward displacement, as much as 17 Å (Figure 6b), is found at the cytoplasmic end of TM6 in concert with a slight inward tilt of the extracellular segment (Figure 6a), which is in line with the crystal structures of β_2AR,[48] but only partly conforms to the previously proposed common activation mechanism of the Rhodopsin family ("global toggle switch mechanism") which suggests a "vertical" seesaw movement of TM6.[49] In the cytoplasmic face, an inward motion of TM7 and an upward shift of TM3 are observed as expected (Figure 6b). Comparison among crystal structures of different GPCRs suggests that the extent of the TM6 motion varies, and the movements of TM3 and TM7 depend on particular receptor and the binding of different ligands.[50] In our system, the binding of **FW01** contributes to the conserved but also unique conformational changes of 5-HT_{1A}R. First, the side chain of D3.32 bends upward to form a hydrogen bond with protonated nitrogen of the **FW01**, which might count for the upshift of TM3. The carbonyl group in **FW01** is engaged in the hydrogen bond with N7.39 (or Y7.43 at first). As a result, the direct salt bridge between D3.32 and Y7.43 present in the inactive 5-HT_{1A}R is interrupted and mediated by **FW01** instead. Specially, the latter involvement of N7.39 in the stronger hydrogen bond with the carbonyl group of the ligand leads to the outward leaning of the extracellular segment of TM7. TM2, which was supposed to have little displacement, moves outward to accommodate the bulky tail of **FW01**—phenyl and cyclohexyl groups, so that the phenyl ring forms favorable $\pi-\pi$ interactions with Y2.64 and F3.28. Likewise, the substantial out-swing of TM6 is also facilitated by agonist binding. The hydrogen bond interaction with S5.42 is common among monoamine receptor agonists and has been proved to be important for agonist binding and activation.[51,52] Given this, the stable hydrogen bond between the nitrogen atom in the indole ring and S5.42 results in an inward bulge and clockwise rotation of TM5 and then triggers concerting rearrangements of nearby residues like what is observed in β_2AR[48] (Figure 7, R″). The hydrophobic packing interaction, which stabilizes the

dx.doi.org/10.1021/ci400481p | J. Chem. Inf. Model. 2013, 53, 3202−3211

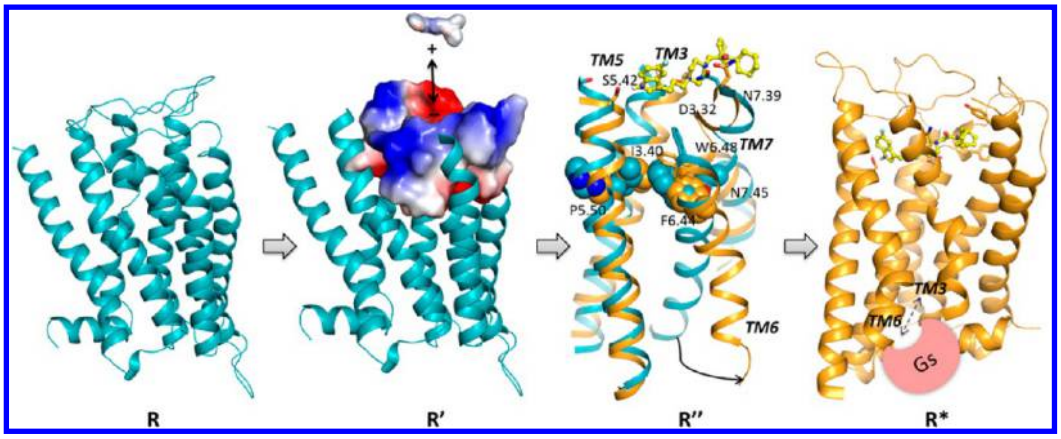

Figure 7. Proposed activation process of 5-HT_{1A}R by an **FW01**-like agonist. R represents the inactive state; R′ depicts the recognition of an agonist driven by electrostatic interaction; R″ presents the agonist binding-induced major structural rearrangements (agonist-bound state, orange cartoon; ligand-free state, cyan cartoon); and R* refers to the fully activated 5-HT_{1A}R coupling with Gs protein (pink). (R* is a schematic diagram, and R″ was taken to represent R* since our simulation does not involve Gs protein.)

relative position of TM3, TM5, and TM6 of 5-HT_{1A}R in an inactive state, is interrupted by the motion of P5.50. As a result, I3.40 and F6.44 are repositioned, and the switch of F6.44 causes a corresponding swing of TM6. Whereas unlike in β_2AR, W6.48 moves distinctly toward P5.50 upon agonsit binding. So W6.48 might play a similar role as a "rotamer toggle switch" in the Rhodopsin receptor[53] that initiates the displacement of F6.44 and I3.40 vice versa. Therefore, in the case of 5-HT_{1A}R, Ser5.42 and W6.48 probably undergo synergy in the process of promoting a large TM6 motion. Eventually, TM6 dramatically moves outward as much as 17 Å.

Proposed Activation Mechanism of 5-HT_{1A}R. On the basis of our MD simulations study and generally accepted knowledge about the activation mechanism of other Family A GPCRs members, a stepwise activation process model of 5-HT_{1A}R was further proposed (Figure 7). Typically, unbounded 5-HT_{1A}R adopts the inactive or basal active state R through its intramolecular interaction and trasits between several energy minima conformations by molecular thermodynamic motion or its inherent flexibility. When protonated **FW01** diffuses to the extracullar mouth of the binding cavity of 5-HT_{1A}R, the electrostatic attraction between the negatively charged region of 5-HT_{1A}R and positively charged **FW01** motivates the ligand recognition and binding process (R′). Then **FW01** is stably cradled in the extracellar segments of TM3, TM5, TM6, and TM7 through several anchoring interactions with D3.32, S5.42, and N7.39. These residues, which in turn act like molecular triggers, propagate the conformational changes to the inner-middle part of the seven bundles: P5.50, I3.40, F6.44, F6.48, and N7.45 are repositioned to form hydrophobic stacking and ultimately translate into a large-scale outward swing of TM6 in the cytoplasmic end (R″). At this stage, the cytoplasmic ends of TM3 and TM6 are largely separated, and 5-HT_{1A}R is ready to bind Gs protein, leading itself to a fully activated state R*.

CONCLUSION

The dynamic pharmacophore model for 5-HT_{1A}R which incorporates the receptor flexibility was built here by integrating a set of computational approaches including homology modeling, molecular dynamics simulation, GROMOS conformational cluster analysis, GRID mapping, and dynamical pharmacophore virtual screening. Finally, through our dynamic pharmacophore based virtual screening protocol, 10 new 5-HT_{1A}R agonists were successfully identified. Three of them reveal high potency of K_i values less than 100 nM. These compounds deserve further considerations for the development of 5-HT_{1A}R "superagonists" through several rounds of structural optimization and QSAR studies. In addition, the investigation of the binding mode of **FW01** with 5-HT_{1A}R provides molecular information for us to improve our pharmacophore model and perform more productive virtual screening. Through MD simulations study, we uncovered unique conformational changes of 5-HT_{1A}R induced by agonist **FW01**. Finally, a stepwise activation model of 5-HT_{1A}R induced by **FW01**-like agonists was proposed. This model can help better the understanding of the signal transduction process from the extracellular side to the cytoplasmic end of 5-HT_{1A}R when activated by exogenous agonists and guide future structure-based agonist design.

ASSOCIATED CONTENT

Supporting Information

Figure S1. This material is available free of charge via the Internet at http://pubs.acs.org.

AUTHOR INFORMATION

Corresponding Authors

*E-mail: hljiang@mail.shcnc.ac.cn. Corresponding author address: Shanghai Institute of Materia Medica, Chinese Academy of Sciences, Shanghai 201203, China (H.J.).

*E-mail: Zhenxuechu@suda.edu.cn. Corresponding author address: Department of Pharmacology, Soochow University College of Pharmaceutical Sciences, Suzhou 215123, China (X.Z.).

*Phone: +86-21-51980010. Fax: +86-21-51980010. E-mail: wfu@fudan.edu.cn. Corresponding author address: Department of Medicinal Chemistry, School of Pharmacy, Fudan University, 826 Zhangheng Road, Shanghai 201203, P.R. China (W.F.).

Author Contributions

§Lili Xu, Shanglin Zhou, and Kunqian Yu contributed equally to this work.

Notes

The authors declare no competing financial interest.

■ ACKNOWLEDGMENTS

This work was supported by the National Natural Science Foundation of China (No. 81172919, 81130023, 30825042) and grants from the State Key Laboratory of Drug Research, the National High Technology Research and Development Program of China (863 Program) (No. 2012AA020301), the State Key Program of Basic Research of China grant (2009CB918502, 2010CB912601, 2009CB522000, and 2011CB5C4403), the State Key Laboratory of Drug Research, and National Drug Innovative Program (No .2009ZX09301-011). Support from Priority Academic Program Development of Jiangsu Higher Education Institutes (PAPD) is also appreciated.

■ REFERENCES

(1) Zifa, E.; Fillion, G. 5-Hydroxytryptamine receptors. *Pharmacol. Rev.* **1992**, *44*, 401−458.
(2) Hoyer, D.; Martin, G. 5-HT receptor classification and nomenclature: towards a harmonization with the human genome. *Neuropharmacology* **1997**, *36*, 419−428.
(3) Feighner, J. P.; Boyer, W. F. Serotonin-1A anxiolytics: an overview. *Psychopathology* **1989**, *22* (Suppl 1), 21−6.
(4) Blier, P.; de Montigny, C. Current advances and trends in the treatment of depression. *Trends Pharmacol. Sci.* **1994**, *15*, 220−6.
(5) Blier, P.; Ward, N. M. Is there a role for 5-HT1A agonists in the treatment of depression? *Biol. Psychiatry* **2003**, *53*, 193−203.
(6) Shimizu, S.; Tatara, A.; Imaki, J.; Ohno, Y. Role of cortical and striatal 5-HT1A receptors in alleviating antipsychotic-induced extrapyramidal disorders. *Prog. Neuro-Psychopharmacol. Biol. Psychiatry* **2010**, *34*, 877−81.
(7) Nicholson, S. L.; Brotchie, J. M. 5-Hydroxytryptamine (5-HT, serotonin) and Parkinson's disease - opportunities for novel therapeutics to reduce the problems of levodopa therapy. *Eur. Neuropsychopharmacol.* **2002**, *9* (Suppl 3), 1−6.
(8) Soumier, A.; Banasr, M.; Goff, L. K.; Daszuta, A. Region- and phase-dependent effects of 5-HT(1A) and 5-HT(2C) receptor activation on adult neurogenesis. *Eur. Neuropsychopharmacol.* **2010**, *20*, 336−45.
(9) Caliendo, G.; Santagada, V.; Perissutti, E.; Fiorino, F. Derivatives as 5HT1A receptor ligands–past and present. *Curr. Med. Chem.* **2005**, *12*, 1721−53.
(10) Lacivita, E.; Leopoldo, M.; Berardi, F.; Perrone, R. 5-HT1A receptor, an old target for new therapeutic agents. *Curr. Top. Med. Chem.* **2008**, *8*, 1024−34.
(11) Lacivita, E.; Di Pilato, P.; De Giorgio, P.; Colabufo, N. A.; Berardi, F.; Perrone, R.; Leopoldo, M. The therapeutic potential of 5-HT1A receptors: a patent review. *Expert Opin. Ther. Pat.* **2012**, *22*, 887−902.
(12) Middlemiss, D. N.; Fozard, J. R. 8-Hydroxy-2-(di-n-propylamino)-tetralin discriminates between subtypes of the 5-HT1 recognition site. *Eur. J. Pharmacol.* **1983**, *90*, 151−3.
(13) Jann, M. W. Buspirone: an update on a unique anxiolytic agent. *Pharmacotherapy* **1988**, *8*, 100−16.
(14) Reed, C. R.; Kajdasz, D. K.; Whalen, H.; Athanasiou, M. C.; Gallipoli, S.; Thase, M. E. The efficacy profile of vilazodone, a novel antidepressant for the treatment of major depressive disorder. *Curr. Med. Res. Opin.* **2012**, *28*, 27−39.
(15) Shapiro, D. A.; Renock, S.; Arrington, E.; Chiodo, L. A.; Liu, L. X.; Sibley, D. R.; Roth, B. L.; Mailman, R. Aripiprazole, a novel atypical antipsychotic drug with a unique and robust pharmacology. *Neuropsychopharmacology* **2003**, *28*, 1400−11.
(16) Heusler, P.; Palmier, C.; Tardif, S.; Bernois, S.; Colpaert, F. C.; Cussac, D. [(3)H]-F13640, a novel, selective and high-efficacy serotonin 5-HT(1A) receptor agonist radioligand. *Naunyn-Schmiedeberg's Arch. Pharmacol.* **2010**, *382*, 321−30.
(17) Rasmussen, S. G.; DeVree, B. T.; Zou, Y.; Kruse, A. C.; Chung, K. Y.; Kobilka, T. S.; Thian, F. S.; Chae, P. S.; Pardon, E.; Calinski, D.; Mathiesen, J. M.; Shah, S. T.; Lyons, J. A.; Caffrey, M.; Gellman, S. H.; Steyaert, J.; Skiniotis, G.; Weis, W. I.; Sunahara, R. K.; Kobilka, B. K. Crystal structure of the beta2 adrenergic receptor-Gs protein complex. *Nature* **2011**, *477*, 549−55.
(18) Carlson, H. A.; Masukawa, K. M.; Rubins, K.; Bushman, F. D.; Jorgensen, W. L.; Lins, R. D.; Briggs, J. M.; McCammon, J. A. Developing a dynamic pharmacophore model for HIV-1 integrase. *J. Med. Chem.* **2000**, *43*, 2100−14.
(19) Deng, J.; Sanchez, T.; Neamati, N.; Briggs, J. M. Dynamic pharmacophore model optimization: identification of novel HIV-1 integrase inhibitors. *J. Med. Chem.* **2006**, *49*, 1684−92.
(20) Bowman, A. L.; Makriyannis, A. Approximating protein flexibility through dynamic pharmacophore models: application to fatty acid amide hydrolase (FAAH). *J. Chem. Inf. Model.* **2011**, *51*, 3247−53.
(21) Thangapandian, S.; John, S.; Lee, Y.; Kim, S.; Lee, K. W. Dynamic structure-based pharmacophore model development: a new and effective addition in the histone deacetylase 8 (HDAC8) inhibitor discovery. *Int. J. Mol. Sci.* **2011**, *12*, 9440−62.
(22) Altschul, S. F.; Madden, T. L.; Schaffer, A. A.; Zhang, J.; Zhang, Z.; Miller, W.; Lipman, D. J. Gapped BLAST and PSI-BLAST: a new generation of protein database search programs. *Nucleic Acids Res.* **1997**, *25*, 3389−402.
(23) Larkin, M. A.; Blackshields, G.; Brown, N. P.; Chenna, R.; McGettigan, P. A.; McWilliam, H.; Valentin, F.; Wallace, I. M.; Wilm, A.; Lopez, R.; Thompson, J. D.; Gibson, T. J.; Higgins, D. G. Clustal W and Clustal X version 2.0. *Bioinformatics* **2007**, *23*, 2947−2948.
(24) Inc., A. S. *Discovery Studio Modeling Environment*, Release 3.5; Accelrys Software Inc.: San Diego, 2012.
(25) Laskowski, R. A.; Rullmannn, J. A.; MacArthur, M. W.; Kaptein, R.; Thornton, J. M. AQUA and PROCHECK-NMR: programs for checking the quality of protein structures solved by NMR. *J. Biomol. NMR* **1996**, *8*, 477−86.
(26) Jones, G.; Willett, P.; Glen, R. C.; Leach, A. R.; Taylor, R. Development and validation of a genetic algorithm for flexible docking. *J. Mol. Biol.* **1997**, *267*, 727−48.
(27) Ballesteros, J.; Weinstein, H. [19] Integrated methods for the construction of three-dimensional models and computational probing of structure-function relations in G protein-coupled receptors. In Elsevier: 1995; Vol. *25*, pp 366−428.
(28) Hess, B.; Kutzner, C.; van der Spoel, D.; Lindahl, E. GROMACS 4: algorithms for highly efficient, load-balanced, and scalable molecular simulation. *J. Chem. Theory Comput.* **2008**, *4*, 435−447.
(29) Kandt, C.; Ash, W. L.; Peter Tieleman, D. Setting up and running molecular dynamics simulations of membrane proteins. *Methods* **2007**, *41*, 475−488.
(30) Berger, O.; Edholm, O.; Jähnig, F. Molecular dynamics simulations of a fluid bilayer of dipalmitoylphosphatidylcholine at full hydration, constant pressure, and constant temperature. *Biophys. J.* **1997**, *72*, 2002−2013.
(31) Schuttelkopf, A. W.; van Aalten, D. M. PRODRG: a tool for high-throughput crystallography of protein-ligand complexes. *Acta Crystallogr.* **2004**, *D60*, 1355−63.
(32) Frisch, M. J. *Gaussian 09*; Gaussian, Inc.: Wallingford, CT, 2010.
(33) Goodford, P. J. A computational procedure for determining energetically favorable binding sites on biologically important macromolecules. *J. Med. Chem.* **1985**, *28*, 849−57.
(34) Humphrey, W.; Dalke, A.; Schulten, K. VMD: visual molecular dynamics. *J. Mol. Graphics* **1996**, *14* (33−8), 27−8.
(35) Maybridge. http://www.maybridge.com (accessed July 14, 2011). Specs. http://www.specs.net/ (accessed July 14, 2011).
(36) Lipinski, C. A.; Lombardo, F.; Dominy, B. W.; Feeney, P. J. Experimental and computational approaches to estimate solubility and permeability in drug discovery and development settings. *Adv. Drug Delivery Rev.* **2001**, *46*, 3−26.
(37) Zhang, H.; Ye, N.; Zhou, S.; Guo, L.; Zheng, L.; Liu, Z.; Gao, B.; Zhen, X.; Zhang, A. Identification of N-propylnoraporphin-11-yl 5-(1,2-dithiolan-3-yl)pentanoate as a new anti-Parkinson's agent

possessing a dopamine D2 and serotonin 5-HT1A dual-agonist profile. *J. Med. Chem.* **2011**, *54*, 4324−38.
(38) Sun, H.; Zhu, L.; Yang, H.; Qian, W.; Guo, L.; Zhou, S.; Gao, B.; Li, Z.; Zhou, Y.; Jiang, H.; Chen, K.; Zhen, X.; Liu, H. Asymmetric total synthesis and identification of tetrahydroprotoberberine derivatives as new antipsychotic agents possessing a dopamine D(1), D(2) and serotonin 5-HT(1A) multi-action profile. *Bioorg. Med. Chem.* **2013**, *21*, 856−68.
(39) Trzaskowski, B.; Latek, D.; Yuan, S.; Ghoshdastider, U.; Debinski, A.; Filipek, S. Action of molecular switches in GPCRs–theoretical and experimental studies. *Curr. Med. Chem.* **2012**, *19*, 1090−109.
(40) Arvidsson, L. E.; Hacksell, U.; Nilsson, J. L.; Hjorth, S.; Carlsson, A.; Lindberg, P.; Sanchez, D.; Wikstrom, H. 8-Hydroxy-2-(di-n-propylamino)tetralin, a new centrally acting 5-hydroxytryptamine receptor agonist. *J. Med. Chem.* **1981**, *24*, 921−3.
(41) Ho, B. Y.; Karschin, A.; Branchek, T.; Davidson, N.; Lester, H. A. The role of conserved aspartate and serine residues in ligand binding and in function of the 5-HT1A receptor: a site-directed mutation study. *FEBS Lett.* **1992**, *312*, 259−62.
(42) Javitch, J. A.; Ballesteros, J. A.; Weinstein, H.; Chen, J. A cluster of aromatic residues in the sixth membrane-spanning segment of the dopamine D2 receptor is accessible in the binding-site crevice. *Biochemistry* **1998**, *37*, 998−1006.
(43) Prandi, A.; Franchini, S.; Manasieva, L. I.; Fossa, P.; Cichero, E.; Marucci, G.; Buccioni, M.; Cilia, A.; Pirona, L.; Brasili, L. Synthesis, biological evaluation, and docking studies of tetrahydrofuran-cyclopentanone- and cyclopentanol-based ligands acting at adrenergic alpha(1)- and serotonine 5-HT1A receptors. *J. Med. Chem.* **2012**, *55*, 23−36.
(44) Nowak, M.; Kolaczkowski, M.; Pawlowski, M.; Bojarski, A. J. Homology modeling of the serotonin 5-HT1A receptor using automated docking of bioactive compounds with defined geometry. *J. Med. Chem.* **2006**, *49*, 205−14.
(45) Güner, O. F.; Henry, D. R. Metrics for Analyzing Hit Lists and Pharmacophores. In *Pharmacophore Perception, Development, and Use for Drug Design*; International University Line: 2000; pp 193−211.
(46) Gaulton, A.; Bellis, L. J.; Bento, A. P.; Chambers, J.; Davies, M.; Hersey, A.; Light, Y.; McGlinchey, S.; Michalovich, D.; Al-Lazikani, B.; Overington, J. P. ChEMBL: a large-scale bioactivity database for drug discovery. *Nucleic Acids Res.* **2012**, *40*, D1100−7.
(47) Mysinger, M. M.; Carchia, M.; Irwin, J. J.; Shoichet, B. K. Directory of useful decoys, enhanced (DUD-E): better ligands and decoys for better benchmarking. *J. Med. Chem.* **2012**, *55*, 6582−6594.
(48) Rasmussen, S. G. F.; Choi, H.-J.; Fung, J. J.; Pardon, E.; Casarosa, P.; Chae, P. S.; DeVree, B. T.; Rosenbaum, D. M.; Thian, F. S.; Kobilka, T. S.; Schnapp, A.; Konetzki, I.; Sunahara, R. K.; Gellman, S. H.; Pautsch, A.; Steyaert, J.; Weis, W. I.; Kobilka, B. K. Structure of a nanobody-stabilized active state of the [bgr]2 adrenoceptor. *Nature* **2011**, *469*, 175−180.
(49) Schwartz, T. W.; Frimurer, T. M.; Holst, B.; Rosenkilde, M. M.; Elling, C. E. Molecular mechanism of 7TM receptor activation–a global toggle switch model. *Annu. Rev. Pharmacol. Toxicol.* **2006**, *46*, 481−519.
(50) Katritch, V.; Cherezov, V.; Stevens, R. C. Structure-function of the G protein-coupled receptor superfamily. *Annu. Rev. Pharmacol. Toxicol.* **2013**, *53*, 531−56.
(51) Chanda, P. K.; Minchin, M. C.; Davis, A. R.; Greenberg, L.; Reilly, Y.; McGregor, W. H.; Bhat, R.; Lubeck, M. D.; Mizutani, S.; Hung, P. P. Identification of residues important for ligand binding to the human 5-hydroxytryptamine1A serotonin receptor. *Mol. Pharmacol.* **1993**, *43*, 516−20.
(52) Liapakis, G.; Ballesteros, J. A.; Papachristou, S.; Chan, W. C.; Chen, X.; Javitch, J. A. The forgotten serine: a critical role for Ser-2035.42 in ligand binding to and activation of the *β*2-adrenergic receptor. *J. Biol. Chem.* **2000**, *275*, 37779−37788.
(53) Shi, L.; Liapakis, G.; Xu, R.; Guarnieri, F.; Ballesteros, J. A.; Javitch, J. A. Beta2 adrenergic receptor activation. Modulation of the proline kink in transmembrane 6 by a rotamer toggle switch. *J. Biol. Chem.* **2002**, *277*, 40989−96.